Available online at www.sciencedirect.com
SCIENCE DIRECT®
Journal of Pharmaceutical and Biomedical Analysis 36 (2004) 211–218
JOURNAL OF PHARMACEUTICAL AND BIOMEDICAL ANALYSIS
www.elsevier.com/locate/jpba

Short communication

Analysis of fluorescence excitation–emission matrix of multicomponent drugs
A case study with human placental extract used as wound healer

Piyali Datta, Debasish Bhattacharyya*

Department of Drug Design, Development and Molecular Modeling, Indian Institute of Chemical Biology, 4 Raja S.C. Mallick Road, Jadavpur, Calcutta 700032, India

Received 23 March 2004; received in revised form 19 May 2004; accepted 19 May 2004

Abstract

The possibility of finger printing of multi component drugs, where a number of components are fluorescent, has been explored after generation of excitation–emission matrix (EEM) contour plots. With nicotinamide adenine dinucleotide, reduced form (NADH) and *N*-acetyl tryptophanamide (NATA) serving as reference compounds, the contour widths were found to be proportional to fluorophore concentration. EEM generated from different batches of processed human placental extract, used as wound healer, in presence and absence of extraneous fluorescence probes like 1-anilino 8-naphthalenesulphonic acid (1-ANS) or dansyl chloride were found to be highly consistent. Variation of contour widths of these EEM after excitation at 280 or 340 nm were essentially zero subject to the limit of detection of variation ($n = 5$). This high degree of consistency between batches has been supported from analysis with such independent techniques like UV-absorption spectra, Fourier Transformed IR spectra, TLC and reverse phase HPLC. The advantages of EEM analysis have been discussed.

Keywords: Fluorescence compounds; Excitation–emission matrix; Drug analysis; Placental extract

1. Introduction

Parallel to synthetic and semi-synthetic drugs of well-defined structure and composition, many partially purified natural products are used for therapeutic purposes. Finger printing of the products is an important feature to ensure its limit of variation particularly of the bioactive molecules. Since there is no fingerprinting technique, which could be applied universally to separate all components, combination of different modes are used and up gradation of finger printing procedures is an active area of research.

Fluorescence spectroscopy has versatile application in chemistry and biochemistry. Modern versions of spectrofluorimeters are equipped with generation of three-dimensional (3D) contour plots, also called excitation–emission matrix or EEM plots, where the *z*-axis represents emission intensity. Its advantage lies on presentation of chromophores having different excitation and emission patterns in a single profile. In analytical chemistry it is frequently used in environmental and hydrological studies ([1,2], reviewed in [3]). Moreover, since wide excitation and emission zones are covered in a single profile, there is no scope of missing any newly emerged fluorophore in a batch. This safe guard is almost impossible to include in two-dimensional fluorescence emission profiles. Here it has been investigated whether similar 3D contour plots could be used for fingerprinting of multi component drugs.

As a case study, human placental extract marketed as a licensed drug has been tested. The extract is used as biological dressing in post-surgical operation and in burn injury [4,5]. Placenta being a rich source of many biologically active components, the extract contains carried over amino acids, peptides, proteins, polynucleotides, lipids and other small bio-organic compounds which are either fluorescent or interacts with external fluorescent probes [6–8]. Thus it was expected that the drug was liable to yield characteristic contour plots suitable for EEM analysis. Using

* Corresponding author. Tel.: +91 33 2473 3491x164; fax: +91 33 473 0284/5197.
E-mail addresses: p_datt@rediffmail.com (P. Datta), debasish@iicb.res.in (D. Bhattacharyya).

0731-7085/$ – see front matter © 2004 Elsevier B.V. All rights reserved.
doi:10.1016/j.jpba.2004.05.006

standard fluorophores, the EEM were calibrated; thus permitting quantification of the components to be analyzed. Considering time management in analysis and data handling, sensitivity and instant identification of an unusual fluorophore in a batch, generation of EEM appeared to be superior to conventional ways of analysis like TLC or HPLC. Validity of the results from EEM was crosschecked by different spectroscopic and chromatographic modes.

2. Experimental

2.1. Reagents

A hot and cold aqueous extract of human placenta manufactured by M/s Albert David Ltd., Calcutta, India and sold under the trade name 'Placentrex' was used. Overall manufacturing procedure holding confidentiality of the proprietary terms has been described recently [8]. *N*-Acetyl tryptophanamide (NATA, $\varepsilon_{280\,nm} = 5.58 \times 10^3\,M^{-1}\,cm^{-1}$), nicotinamide adenine dinucleotide, reduced form (NADH, $\varepsilon_{340\,nm} = 6.3 \times 10^3\,M^{-1}\,cm^{-1}$), 1-anilino 8-naphthalene-sulphonic acid (1-ANS, $\varepsilon_{350\,nm} = 5.0 \times 10^3\,M^{-1}\,cm^{-1}$) and dansyl chloride (DNS-Cl, $\varepsilon_{340\,nm} = 4.5 \times 10^3\,M^{-1}\,cm^{-1}$) were from Sigma, USA. Ethanol (dehydrated alcohol, Bengal Chemical and Pharmaceutical Ltd., Calcutta), methanol (HPLC grade, SRL, Bombay) and ethyl acetate (GR, E. Merck) were used. Water was purified by Milli-Q-Plus system (Millipore).

2.2. Generation of excitation–emission matrix

All contour plots were generated with a Hitachi F 4500 spectrofluorimeter under the following instrumental conditions: excitation and emission wavelength ranges, 240–600 and 240–800 nm, respectively; excitation and emission silt widths, 5 nm each; sampling interval, 5 nm each; scan speed, 12,000 nm/min; contour interval, 5 and contour plots were generated at 100 intensity units. For convenience, the matrix was divided into grids A–D (vertical) and 1–3 (horizontal). A quartz cuvette of 3 ml capacity with Teflon lid holding 2 ml of sample was used and its orientation in cuvette holder was not altered. Concentrations of the fluorophores were varied by replacing solvent in the cuvette. Temperature of the cuvette was maintained at 25 ± 1 °C by a circulating water bath (Polyscience, USA).

2.3. UV-absorption spectra

Optical absorbance was measured with a digital UV–vis spectrophotometer (Digispec-200 GL, SICO, India). Absorption spectra were scanned between 240 and 450 nm with a Specord 200 (Analytical Jena, Germany) recording spectrophotometer between 25 and 28 °C. Scan speed was 50 nm/s and deuterium (UV)–tungsten (VIS) lamp change occurred at 340 nm. Placental extract (1 ml) as supplied was used for scanning. Auto zero correction in the said spectral zone was done with water.

2.4. Fourier transformed (FT)-IR

Placental extract (1 ml) from different batches were evaporated to dryness and were reconstituted with KBr as pallets. FT-IR spectrum was scanned with a Jasco FT-IR 410 model and an average of five scans per sample was recorded. In all sets, corrections were done with air serving as blank.

2.5. TLC and HPTLC

TLC were done with four solvent system: (a) ethanol:ethyl acetate:water (70:20:10 (v/v/v)); (b) ethanol:methanol (80:20); (c) ethanol:methanol:ethyl acetate:water (50:30:10:10); and (d) ethanol:methanol:water (80:10:10) using 10 × 5 cm silica gel 60 F_{254} aluminium impregnated TLC sheets (Merck, Germany). Chromatograms were developed at 28 °C and the spots were viewed under short wavelength UV irradiation at 254 nm by mineralight lamp (model no. UVGL-25, UVP, Upland, CA, USA). A Camag instrument (Scanner 3) was used for HPTLC analysis on 20 × 10 cm silica gel impregnated over aluminium sheets (Merck) where distance between tracks were 10 mm. Spots were viewed by deuterium lamp at 254 nm and their quantification was done by Camag software no. (c)-1998. Placental extract was concentrated 20-fold under vacuum from which 4 and 20 μl were applied on TLC and HPTLC plates, respectively. Concentration of the drug did not leave any precipitation or turbidity.

2.6. HPLC

Placental extract was analyzed using Waters reversed phase C_{18} μ-Bondapak analytical column (7.8 mm × 300 mm; 125 Å, 10 μm) isocratically where the column was equilibrated and eluted with 10 mM K–phosphate, pH 7.5 at a flow rate of 1.0 ml/min. Alternately, the column was equilibrated with water containing 0.1% TFA and a linear gradient of water–80% acetonitrile each containing 0.1% TFA was applied during 30 min at a flow rate of 1.0 ml/min. Elution was monitored at 220 nm. In all sets, 10 μl of placental extract was applied. Blank runs with water served as control where no spurious peaks appeared.

2.7. Other methods

Interaction of ANS with the placental extract in presence of 20 mM K–phosphate, pH 7.5 (1:1 (v/v)) was followed after incubating with 50 μM of the reagent for 15 min at ambient temperature before analysis. DNS-Cl (50 μl from an acetone solution of 1 mg/ml) was added to 1 ml of the placental extract in the said buffer (1:1 (v/v)) and was incubated at 25 °C for 16 h before analysis. Aqueous solution of ANS and DNS-Cl at identical concentration served as control.

Minor precipitate of hydrolyzed products of DNS-Cl or denatured proteins was removed by low speed centrifugation.

3. Results

3.1. Characterization of EEM

The excitation–emission matrix generated with distilled water, 60 μM of NATA, 20 μM of NADH and a mixture of said proportion of NATA and NADH have been presented in Fig. 1. The matrix of NATA shows strong emission in D1 that is typical of tryptophan (ex: 280 nm; em: 300–400 nm). Similarly NADH shows strong emission in D2 that is non-specific for aromatic compounds together with its characteristic emission centered at 450 nm (C2) (ex: 340 nm; em: 380–500 nm). A spectrum of NATA and NADH together having said concentrations shows additive emissions of the individual components illustrating possibility of identification of multiple fluorophores in a mixture (Fig. 1).

In all EEMs, a prominent emission was marked from D1 to A2 identified as Raleigh's scattering where excitation and emission wavelengths were the same together with weak Raman scattering from water, which ran parallel to Raleigh's in D1 and C1. Raman scattering was clearly visible in the EEM of water. Another fairly strong scattering was visible in all profiles in D2 and was extended up to C3. This second order band was observed even with air as sample. Its origin laid on the fact that after Raleigh's scattering of wavelength λ at 90°, the scattered light was constituted of wavelengths primarily of λ but also of integral multiples of λ like 2λ, 3λ, etc. with exponentially decreasing intensity. This scattering was visible corresponding to wavelength double to Raleigh's one. In all EEM, it was clear that this second order emission existed only when Raleigh's scattering was significant; for example, Raleigh's scattering being prominent with placental extract in C1 compared to water, the second order scattering was extended to C3 for the extract only and was absent for water. Similarly for ANS at 50 μM in water, low intensity of second order scattering in D2 apparently merged with the contour of the reagent as the parent Raleigh's scattering in D1 and C1 were relatively weak (described later). However, when the concentration of ANS was gradually reduced to 5 μM with corresponding reduction of contour

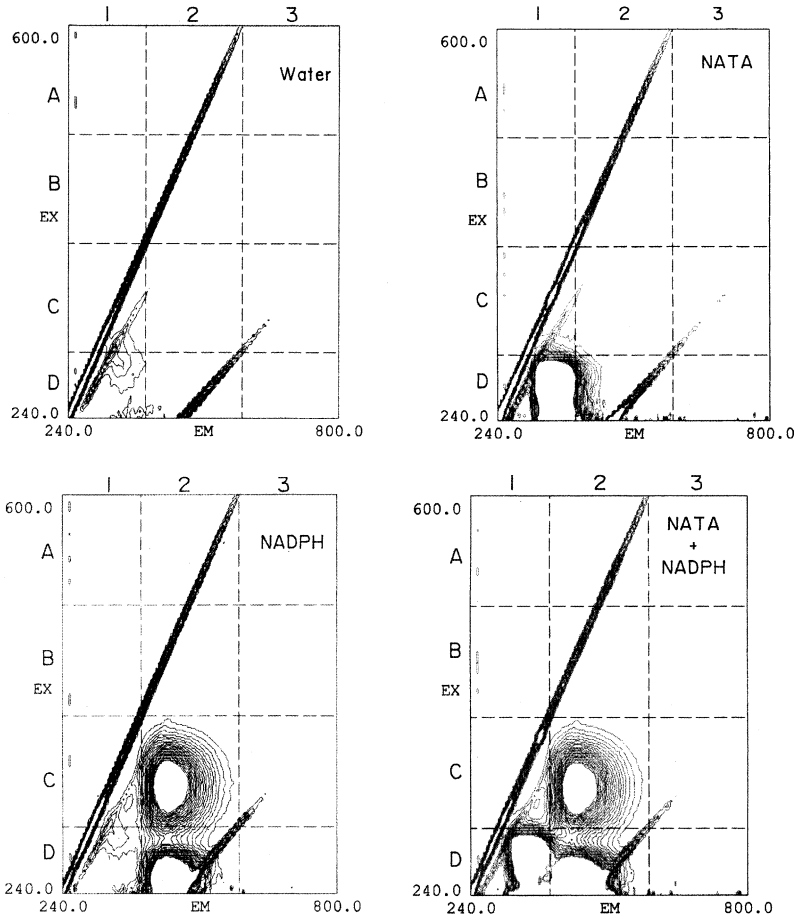

Fig. 1. Excitation–emission contour plots of standard compounds as mentioned in respective panels. Experimental conditions have been mentioned in the text and were maintained throughout. Ex and Em stand for excitation and emission, respectively. Concentrations of NATA and NADH were 60 and 20 μM, respectively.

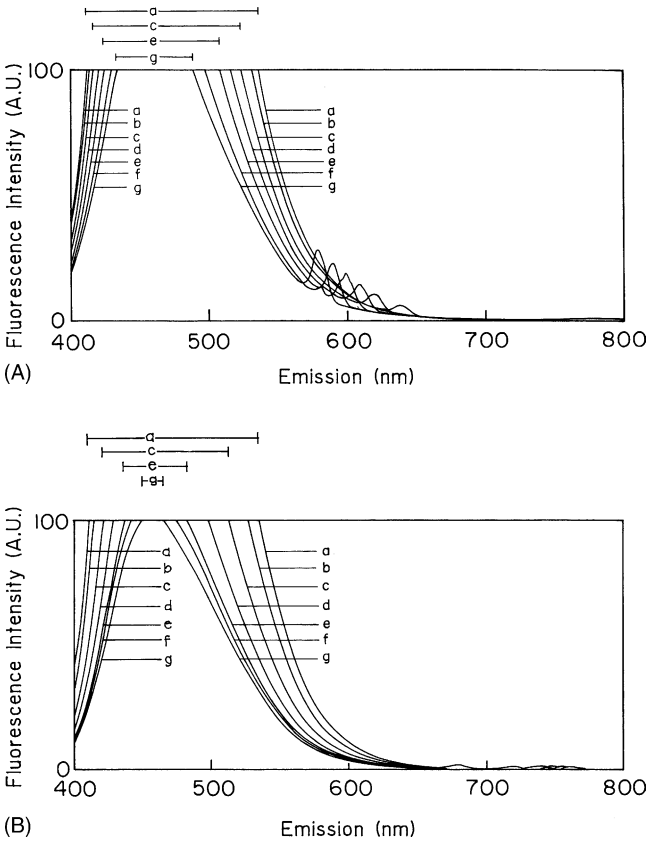

Fig. 2. Two-dimensional emission spectra of 25 μM NADH after excitation between: (A) 290 and 340 nm; and (B) 340 and 380 nm. Excitation maximum of NADH was at 340 nm [8]. Scanning conditions were as par Fig. 1. Contour widths of the spectrum have been marked were measured in centimeters between the points where they are intercepted by the intensity axis at 100. Excitation wavelengths were as follows: in (A) a: 340 nm, b: 320 nm, c: 310 nm, d: 305 nm, e: 300 nm, f: 295 nm, and g: 290 nm; in (B) a: 340 nm, b: 360 nm, c: 370 nm, d: 375 nm, e: 378 nm, f: 379 nm, and g: 380 nm, respectively. Actual measurements from alternate spectra of (A) and (B), i.e., a, c, e and g have been marked on top in either presentation.

widths, the second order scattering reappeared similar to the profile of water. The scattering patterns should also be considered keeping in view of the absorption profile of the test samples leading to 'inner filter effects'. Though the second order emission was mentioned as an artifact in the instrument manual, its origin is now fairly clear. Scatterings have not been, however, considered in the present analysis. Any emission left to Raleigh's scattering is not fluorescence by definition as par 'Jablonsky' diagram.

In order to represent the change of emission pattern with alteration of excitation wavelength with a contour at 100 units of emission (arbitrary units) in a two-dimensional plot, emission from 20 μM of NADH between 400 and 800 nm was followed. Excitation wavelength was changed from 340 nm (excitation maxima) to 290 nm (Fig. 2A) or 380 nm (Fig. 2B). Contour widths were measured in cm from printouts of the two dimensional spectrum. As expected, emission intensity decreased with gradual decrease of contour widths while there was a red or blue shift of excitation wavelength from maximum. Emission patterns where maximum intensity were below 100 were not included in Figs. 2A or B because the contour lengths were 0 for all of them. The dependency of contour width on change of excitation wavelength between 290 and 310 nm was essentially linear but was different in the rest of the excitation zone reflecting the asymmetric pattern of the excitation spectra [8].

Unless self-quenching and/or 'inner filter effects' play roles, fluorescence emission intensity is proportional to fluorophore concentration. Many authors using EEM apply several algorithms, e.g., parallel factor analysis (PARAFAC) for the quantification of compounds from the EEM data [3]. As an alternate approach, EEM were generated with 25–100 μM of tryptophan and 2–30 μM of NADH in water. Contour widths were measured in the scale of emission wavelength from emission spectra using the cursor of the electronic display keeping ordinate maxima at 100 and excitation wavelength at 280 or 340 nm, respectively. This is the most convenient and accurate way to measure contour widths; for example, in the print outs it is almost impossible to locate the emission lines corresponding to say, excitation at 280 or 340 nm. A calibration curve was constructed with tryptophan or NADH concentration with contour width where linear dependence was observed; R^2 (regression coefficient) = 0.999 (tryptophan) and 0.999 (NADH), respectively. A value of $R^2 = 0.999$, i.e., close to 0% variation should be accepted with the assumption that contour lengths could be measured at a minimum difference of 5 nm—a limit set by the instrument parameters.

3.2. EEM of placental extract

EEM of four batches of placental extract, referred as PLX1–4 has been illustrated (Fig. 3). They show tryptophan like emission in D1, NADPH like emission in C2 together with other emissions in B2. Minor spots were observed in D3. However, A3, B3 and C3 grids were free from emissions. Appearance of the four EEMs were very similar suggesting high degree of consistency of relative abundance of fluorophores in the drug ($n = 5$). Also, in none of the EEMs any new contour appeared. Variation of contour widths was quantified after holding the excitation wavelength at 280 or 350 nm where 0% variation was observed ($R^2 = 0.999$).

Further, attempt was made to quantify NADPH content of placental extract assuming identical emission patterns of NADH and NADPH (ex: 340 nm) [8]. Earlier, it has been demonstrated that NADPH of the extract had a red shift of excitation maxima from 340 to 360 nm compared to reference NADPH possibly due to interfering molecules. Therefore contour widths of the drug after excitation at 360 nm was considered and that yielded nucleotide content to be 20–22 μM. This was indeed very close to 20–25 μM as reported earlier [8].

ANS is used as an extraneous fluorescence probe sensing hydrophobic patches of proteins and lipids [9]. The emission

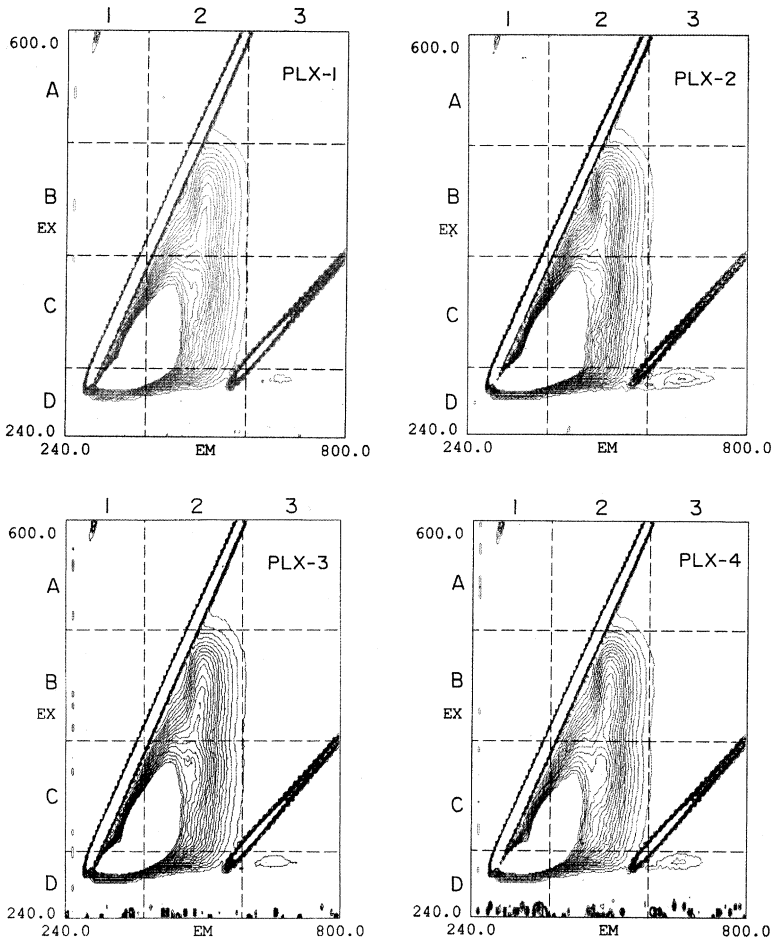

Fig. 3. Excitation–emission contour plots of four batches of placental extract as referred by PLX1–4. Ex and Em stand for excitation and emission, respectively.

matrix of ANS alone or with three batches of the extract (referred as PLX1–3) has been illustrated in Fig. 4. ANS shows weak emission centered at C2. For the extracts, the strong emission centered at C1–D2 crossover point in comparison to Fig. 3 is greatly reduced while new patterns are generated in B2 and C2. This is partly because of 'charge transfer complex' formed by aromatic residues with ANS [10,11]. This results in partial quenching of aromatic residue emission as ANS abstracts a part of the emitted quantum [12]. Once again, the emission matrix of different batches of the extract was found to be highly consistent having a center of contour at B–C grid line. The contour widths were measured from emission spectrum after excitation at 375 nm having ordinate maxima at 100 where no variation was detected (R^2 = 0.999).

DNS-Cl reacts with primary amines, amino acids, peptides and proteins yielding fluorescence compounds [13]. Different batches of the extract were allowed to react with DNS-Cl and contour plots were generated. Though a major portion of contour area overlapped with the extract's original pattern, once again, variation of contour widths was insignificant (R^2 = 1.000). This high degree of consistency among batches of placental extract was crosschecked by other modes as described below.

3.3. UV-absorption spectra

A 20-fold diluted placental extract with water after base line corrections revealed absorption maxima at 256.1 ± 0.1 nm having absorbance of 0.681 ± 0.015 (n = 6). Superimposed spectra of four batches have been shown in Fig. 5. Weak but significance absorption of the undiluted drug between 300 and 400 nm with a monotonous decrease of intensity has been reported earlier [8].

3.4. FT-IR

Analysis of FT-IR profiles of dried placental extract between 4000 and 400 cm^{-1} showed occurrence of the following major bands: a broad hump centered at 3426 ± 2 cm^{-1} together with prominent signals at 1634, 1596, 1408 ± 2, 1119, 1081 and 534 ± 1 cm^{-1} (n = 6) (variation of peak positions within 1 cm^{-1} has not been mentioned). While the 3426 cm^{-1} band has been assigned to OH and/ NH stretching frequency (which varies between 3700 and 3100 cm^{-1}),

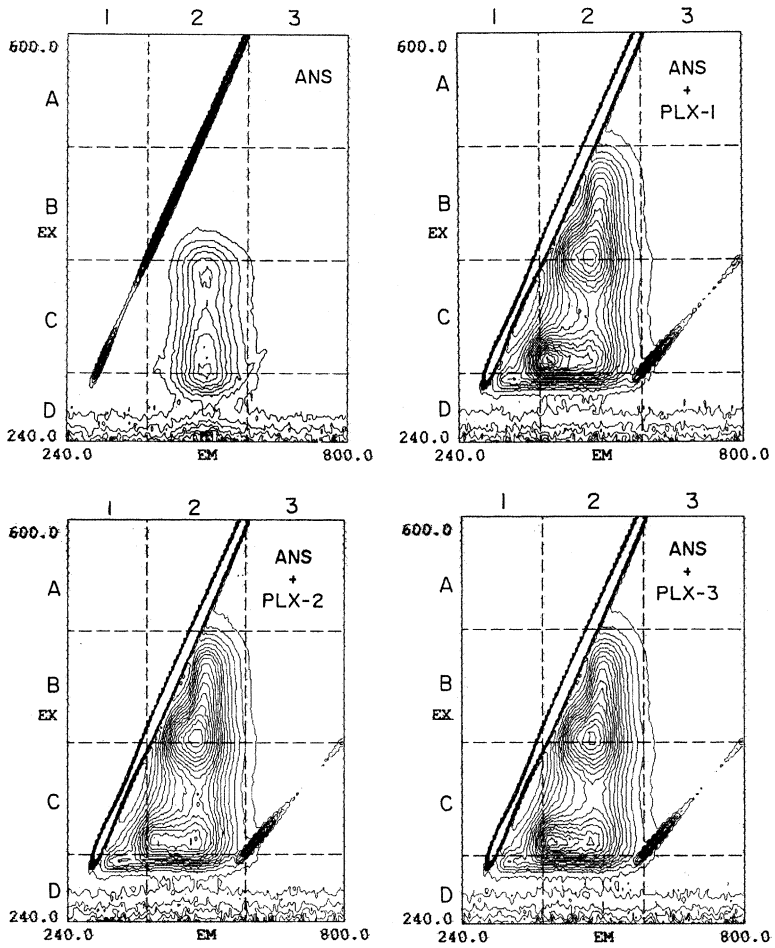

Fig. 4. Excitation–emission contour plots of ANS in absence and presence of three batches of 'Placentrex' referred as ANS or PLX1–3, respectively. Ex and Em stand for excitation and emission, respectively.

the 1634, 1595 and 534 cm^{-1} bands are normally assigned to amide stretching (primarily from polypeptides), aromatic residues and $(CH_2)_n$ rocking, respectively.

3.5. TLC and HPTLC

TLC analysis of placental extract with silica gel using four solvent systems revealed separation of three to four major and one to two minor spots. R_f of the spots in different solvents have been summarized in Table 1 ($n = 4$). To quantify relative abundance of the spots, some of the analyses were performed with HPTLC (Table 2) ($n = 4$). Maximum variation of R_f and abundance of spots between different batches

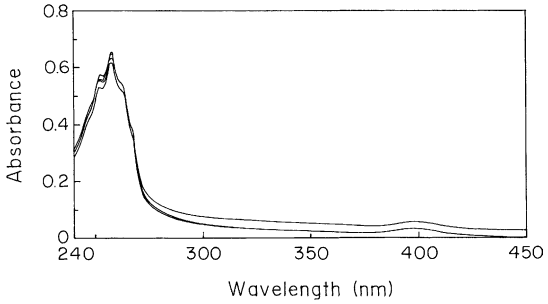

Fig. 5. Superimposed UV-absorption spectra of 20-fold diluted placental extract in water between 240 and 450 nm ($n = 4$).

Table 1
Silica gel TLC profiles of placental extract ($n = 4$)

Solvent system	R_f
Ethanol:ethyl acetate:water (70:20:10)	0.61 ± 0.01, 0.71 ± 0.01, 0.85 ± 0.01
Ethanol:methanol (80:20)	0.54 ± 0.02, 0.69 ± 0.02, 0.85 ± 0.02
Ethanol:methanol:ethyl acetate:water (50:30:10:10)	0.59 ± 0.01, 0.63 ± 0.02, 0.77 ± 0.02

Table 2
Silica gel HPTLC profiles of placental extract ($n = 4$)

Solvent system	R_f	Abundance (%)
Ethyl acetate:acetic acid:water (10:10:80)	0.08 ± 0.00	7.2 ± 1.3
	0.35 ± 0.01	27.5 ± 1.4

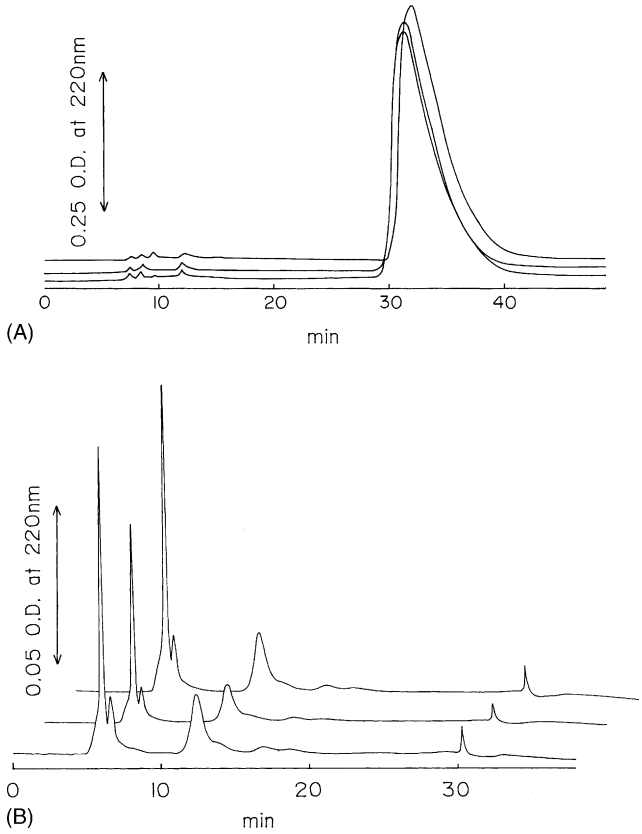

Fig. 6. Overlapping HPLC profiles of placental extract ($n = 3$) using C_{18} reversed phase column (A) under isocratic elution in presence of 20 mM Na–phosphate, pH 7.5 at a flow rate of 1 ml/min and (B) water–80% acetonitrile gradient containing 0.1% TFA at the same flow rate. Elution was followed at 220 nm ($n = 3$). To check reproducibility of retention times with sample volumes, one of the samples was loaded 60% to the others.

of the extract was limited between ±0.02 and ±5%, respectively.

3.6. HPLC

The extracts were further analyzed by RP-HPLC using two different modes; under isocratic condition in presence of low salt buffer and under a linear gradient of water–methanol for 30 min where nucleotides and peptides including small organic molecules were expected to be eluted, respectively [8,14–16] (Fig. 6A and B) ($n = 3$). In the isocratic elution, several peaks of very low abundance were observed around 10 min (retention time, $R_t = 7.47 \pm 0.02$ min, relative abundance, RA $= 0.10 \pm 0.02\%$; $R_t = 8.51 \pm 0.02$ min, RA $= 0.20 \pm 0.03\%$; $R_t = 9.50 \pm 0.01$ min, RA $= 0.22 \pm 0.20\%$; $R_t = 12.33 \pm 0.03$ min, RA $= 0.45 \pm 0.04\%$ ($n = 4$). The major component was eluted at $R_t = 32.56 \pm 0.52$ min having abundance of $99.1 \pm 0.20\%$. In separate studies it was observed that this peak was largely constituted of polynucleotides of different sizes ([17], also P. Datta, unpublished observations). Variation of composition of the polynucleotide mixture probably induced a degree of variation of R_t of this peak compared to others. In the gradient elution, the following peaks were observed ($n = 6$): $R_t = 6.06 \pm 0.01$ min, RA $= 54 \pm 0.32\%$; $R_t = 6.61 \pm 0.01$ min, RA $12.37 \pm 0.04\%$; $R_t = 12.35 \pm 0.01$ min, RA $29.45 \pm 0.10\%$; and $R_t = 30.25 \pm 0.01$ min, RA $3.6 \pm 0.2\%$.

4. Discussions

Among various modes of finger printing of drugs, generation of EEM of its fluorescence components offers a convenient way to check batch variations. The advantages are—a modern version of laboratory spectrofluorimeter is capable of producing such matrix in about 5 min, non-destructive, sensitive in the range of 5 μM—5 mM of fluorophores depending on quantum yield, highly reproducible and free from manual error (Fig. 1). Their applicability may be broadened after application of external fluorescence probes. Further, the contours could quantify fluorophores.

Based on probable composition of placental extract [6,7], EEM matrix was generated from its different batches. In presence and absence of extraneous fluorescence probes, variation of contour widths was <1% and in no batch additional or unusual contours have been observed (Figs. 3 and 4). It is also noteworthy that in the EEM of Fig. 3 or Fig. 4, no unique spot appeared for a particular batch. This degree of consistency was crosschecked by such independent spectroscopic and chromatographic techniques like UV-absorption spectra, FT-IR, TLC, HPTLC and HPLC (Tables 1 and 2, Figs. 5 and 6). Results presented assert that batches of placental extract are indeed well consistent and thus the EEM contours are true expression of this consistency. This consistency reflects standardization of the manufacturing process of the drug from full term matured placenta, which maintains uniformity of its composition as far as possible irrespective of the nutritional status of the mother. Also, unwarranted variation of composition of healthy human organs appears to be largely reduced from evolutionary developments.

Acknowledgements

M/s Albert David Ltd., Calcutta funded the research project and a senior research fellowship (P. Datta). Anachrom R&D Laboratory, Bombay provided HPTLC analysis as courtesy. Dr. V.S. Giri together with his associates and Ms. Pritha Maitra provided FT-IR profiles and analysis of second order scattering emission.

References

[1] I.M. Warner, G. Patonay, M.P. Thomas, Anal. Chem. 57 (1985) 463A.
[2] L.B. McGown, F.B. Bright, Anal. Chem. 56 (1984) 1400A.

[3] M.C. Goldberg, E.R. Weiner, in: O.S. Wolfbeis (Ed.), Fluorescence Spectroscopy—New Methods and Applications, Springer-Verlag Publications, 1993, pp. 213–241.
[4] S.G. Honavar, A.K. Bansal, V.S. Sangwan, G.N. Rao, Opthalmology 107 (2000) 975–979.
[5] K.M. Ramakrishnan, V. Jayaraman, Burns 23 (1997) 33–36.
[6] H. Pande, J. Calaycay, D. Hawke, Ben-Avram, J.E. Schively, J. Biol. Chem. 260 (1985) 2301–2306.
[7] D.J. Wang, N. Huang, L.A. Heppel, Biochem. Biophys. Res. Commun. 166 (1990) 251–258.
[8] P. Datta, D. Bhattacharyya, J. Pharm. Biomed. Anal. 34 (2004) 1091–1098.
[9] J. Slavik, Biochem. Biophys. Acta 694 (1982) 1–25.
[10] J.R. Lakowicz. Principles of Fluorescence Spectroscopy, Planum Press, New York, 1983, pp. 187–215.
[11] E. Haas, in: H.A. Havel (Ed.), Spectroscopic Methods for Determining Protein Structure in Solution, VCH Publications Inc., 1996, pp. 28–61.
[12] D. Amir, S. Krause, E. Haas, Proteins Struct. Funct. Genet. 13 (1992) 162–173.
[13] W.R. Gray, Methods Enzymol. 25 (1972) 121–138.
[14] C.J. Newton, S.M. Faynor, D.B. Northrop, Anal. Biochem. 132 (1983) 50–53.
[15] S. Dutta, N.R. Maity, D. Bhattacharyya, Eur. J. Biochem. 244 (1997) 407–413.
[16] S. Nayar, A. Brahma, B. Barat, D. Bhattacharyya, Biochemistry (2004) (in press).
[17] G. Tonello, M. Daglio, N. Zaccarelli, E. Sottofattori, M. Mazzei, A. Balbi, J. Pharma. Biomed. Anal. 14 (1996) 1555–1560.